

Surface modification affect the biodistribution and toxicity characteristics of iron oxide magnetic nanoparticles in rats

ISSN 1751-8741

Received on 7th July 2017

Revised 12th December 2017

Accepted on 9th January 2018

E-First on 23rd April 2018

doi: 10.1049/iet-nbt.2017.0152

www.ietdl.org

Pengfei Yang¹, Hengyi Xu¹ , Zhihong Zhang¹, Lin Yang¹, Huijuan Kuang¹, Zoraida P. Aguilar²

¹State Key Laboratory of Food Science and Technology, Nanchang University, 235 Nanjing East Road, Nanchang 330047, People's Republic of China

²Zystein, LLC, Fayetteville, AR 72704, USA

 E-mail: kidyxu@163.com

Abstract: Various surface modifications of iron oxide magnetic nanoparticles (IOMNs) can improve their stability and long-term retention time *in vivo*, expanding applications of biomedical fields. However, whether the long-term retention of IOMNs coated with different surface modifications has toxic effects remains poorly understood. Here, the toxicity of IOMNs modified with polyethylene glycol (PEG), bovine serum albumin (BSA), and carboxyl group (COOH), forming PEG-IOMNs, BSA-IOMNs, and COOH-IOMNs, respectively, were evaluated in the rats. The high accumulation of PEG-IOMNs and COOH-IOMNs both in the liver and lung, and the high accumulation BSA-IOMNs in blood after 24 day recovery were observed by elemental content analysis. Except individual neutrophils in the local portal area, PEG-IOMNs can also induce cytoplasmic vacuolisation in partial liver cells by histopathological examination. Furthermore, the results of RT-qPCR showed that PEG-IOMNs, BSA-IOMNs, and COOH-IOMNs can change the transcript levels of most genes related to iron homeostasis, mitochondria apoptosis, inflammatory response, but <2-fold alteration. COOH-IOMNs seemed to induce normal cell apoptosis more easily than BSA-IOMNs and PEG-IOMNs. In conclusion, BSA-IOMNs had longer-term retention time in blood. IOMNs coated with PEG and BSA can still induce side effects on the liver.

1 Introduction

Iron oxide magnetic nanoparticles (IOMNs) provide an alternative method of drug delivery, cancer therapy, and magnetic resonance imaging with the development of nanotechnology [1, 2]. Nevertheless, previous studies demonstrated that IOMNs can trigger cytotoxicity *in vitro* [3, 4]. Furthermore, IOMNs could result in toxicity in the liver, kidneys, and lung [5]. Our earlier study also showed that smaller IOMNs (10 and 20 nm) more effectively changed the transcript levels of genes related to oxidant stress, apoptosis in the liver [6]. Hence, surface modification of IOMNs with polyethylene glycol (PEG), polyvinyl alcohol, dextran, and other materials were used to improve the stability and biocompatibility, and diminish the toxicity of IOMNs [7–10].

In addition, IOMNs modified with various materials exhibited different biocompatibility. PEG-coated IOMNs exhibited minimal cellular uptake and highest cell viability compared with polyacrylic acid (PAA) and polyethylenimine (PEI) coated IOMNs, and IOMNs functionalised with PEI showed the most reduction (20%) of cell viability [11]. Silane-PEG-coated IOMNs induced lower ROS production and lower expression of p53 in comparison to IOMNs coated with citric acid, nitric acid, and perchloric acid in liver tissues 24 h post-exposure [12]. Furthermore, studies revealed that IOMNs functionalised with surface coating still induced toxicity. Silva *et al.* [13] reported that IOMNs coated with PEG2000 with different dosage (12.5, 25, and 50 mg/kg) caused vascular congestion, necrosis, and inflammatory infiltrate in the liver and kidneys on the 14th day after intravenous administration. Easo and Mohanan [14] found that dextran stabilised iron oxide nanoparticles (NPs) could induce oxidative stress response in liver at days 1 and 7 after intravenous exposure (10 mg/kg). Therefore, it was essential to evaluate and compare the possible side effects of IOMNs with different surface modification, especially after long-term recovery *in vivo*. However, these researches were not efficient enough.

As two common commercial materials, PEG and bovine serum albumin (BSA) were generally non-toxicity. PEG modification can prolong the half-life of most proteins or drugs in plasma [15], and

BSA was usually used as the model for human serum albumin and ligand to bind various drug species [16]. In addition, studies demonstrated that IOMNs functionalised with PEG exhibited non-specific protein adsorption and increasing circulation time *in vivo* [15, 17, 18]. BSA modification improved the biocompatibility and solubility of IOMNs [19, 20], which enhanced the compatibility of IOMNs with the human body as drug delivery carriers [21, 22]. Meanwhile, studies reported that IOMNs coated with BSA showed less toxicity *in vitro* [23], and PEG modification reduced the acute toxicity of IOMNs in the liver [24].

In this study, we evaluated the bio-distribution and toxicity of three types of IOMNs that were coated with carboxyl group, carboxyl group followed by PEG coating, and carboxyl group followed by BSA coating after 24 days of the recovery period. Toxicological evaluation was evaluated through serum biochemistry, histopathological examination, and alterations of liver gene expression related to apoptosis, iron homeostasis, inflammatory response, and stress response. The results provided valuable information and insights to their future applications in medicine.

2 Materials and methods

2.1 Preparation and characterisation of IOMNs

IOMNs in the form of Fe_3O_4 decorated with carboxylic acid, -COOH, forming COOH-IOMNs, were supplied by Ocean NanoTech, LLC (San Diego, CA, USA). The size of COOH-IOMNs was ~40 nm in diameter, and was characterised and confirmed in our previous study [6]. Also, COOH-IOMNs were characterised with JEOL JSM 6701F field emission scanning electron microscopy in the centre of analysis and testing of Nanchang University. These IOMNs were coated with BSA or PEG to form BSA-IOMNs and PEG-IOMNs. Modification with BSA or PEG through covalent conjugation was carried out using the following protocol: 0.5 ml 40 nm COOH-IOMNs (2 mg/ml, dissolved in 0.5 ml borate buffer, 200 mM, pH7) was activated with 0.1 mg of 1-ethyl-3-(3-dimethylaminopropyl)-carbodiimide

hydrochloride (EDC) and 0.1 mg Sulfo-N-hydroxysuccinimide (NHS) at room temperature for 5 min. Then 7 mg BSA or PEG dissolved in 0.5 ml borate buffer (200 mM, pH 7) was added. The reaction was incubated at room temperature for 2 h with continuous stirring. The PEG-IOMNs and BSA-IOMNs NPs were purified using a magnetic separator with a magnetic field gradient of 1.0 T, and the resulting pellet was re-suspended in sterilised PBS containing 0.2% Na₃ and stored at 4°C. The hydrodynamic size of IOMNs was measured with dynamic light scattering using a Zetatracer Ultra 151 (Microtrac Inc., Montgomeryville, PA, USA). To determine the average surface charge on the IOMNs, the zeta potential was also established using the Zetatracer Ultra 151. The formulated particles were also evaluated by the different migration speed by electrophoresis in 1% agarose gel.

2.2 Animals and treatment

Adult male Sprague–Dawley rats (~10 weeks old) of clean grade were obtained from the experimental animal centre of Nanchang University, China. All animals in this experiment were kept at 25°C with a 12 h light/dark cycle; food and water were ad libitum. All procedures involving animals were approved by the Animal Care Review Committee (approval number 0064257), Nanchang University, Jiangxi, China, and adhered to the institutional animal care committee guidelines. After acclimation for 1 week, the animals were used for the study. Three kinds of IOMNs functionalised with different materials were diluted using ultrapure water. Two consecutive tail-vein injections (injected at 0 and 24 h) of the IOMNs (50 mg/kg body weight) were administered to the rats. The dosage was chosen referring to previous study [13]. The weight of the rats, food intake, and physiological behaviours were examined every day. The rats were randomly divided into four groups (five in each group): three treatment groups were exposed to IOMNs functionalised as described above and one control group that was treated with physiological saline. Body weights were recorded every 2 days, and blood samples from the four groups were collected from the orbital venous plexus using a capillary glass tube that pierced the inner canthus without affecting the rats on days 1, 9, 16, and 24 post-injection after being anaesthetised by aether. Also, blood was collected as much as possible on day 24 post-injection at the state of anaesthesia. Blood samples were stored at 4°C for 12 h. Each blood sample (~0.8 ml) was centrifuged at 4000 rpm for 10 min for biochemistry examination. The serum collected was stored at –20°C before use. The liver, spleen, kidneys, heart, lung, intestine, brain, and testis were isolated on day 24 post-injection for visceral index measurement and ion content analysis. A small portion of tissue was stored in RNA fixer stabilisation reagent (RP1302, Lot#0020140902, Biotek Corporation) for 12 h and then stored at –80°C for total RNA extraction. A small part of the liver was fixed in 10% neutral buffered formalin for histopathological examination.

2.3 Elemental content analysis

The small parts of organs used for elemental content analysis were cleaned by physiological saline before collection and digestion. The iron (Fe) contents in the organs (heart, liver, spleen, lung, kidneys, intestine, and testis) were analysed by atomic absorption spectroscopy (AAS, TAS-990, Beijing Purkinje General Instrument Co. LTD). A small amount of each organ (0.2–0.5 g) was dissolved in digestion solution (HNO₃: 10 ml; HClO₄: 2 ml) and were heated to 230°C. The temperature was increased to 280°C when the reaction reached equilibrium. Digested organ samples were diluted with ultrapure water to 25 ml after removal from the heating block. Digested organ samples were used to determine the iron concentrations using AAS.

2.4 Serum biochemistry

The liver function were evaluated through serum levels of alanine aminotransferase (ALT), aspartate aminotransferase (AST), total bilirubin (TBIL), direct bilirubin (DBIL), total protein (TP), albumin (ALB), globulin (GLB), the ratio of ALB to GLB (A/G), γ

Table 1 Primers selected for RT-qPCR

Gene	Primer	Sequence (5'→ 3')
<i>Cyc</i>	forward	GTCTGTTGGCGGAAGA
	reverse	TGTTCTGTTGGCCTCTGTG
<i>Apaf-1</i>	forward	GTGGAGGTGATCGTGAATG
	reverse	ATGGTGCTGTGATGACCTGT
<i>Caspase-8</i>	forward	TGATTGCACAGCAAGTCAA
	reverse	TAGGATGCAGCAGATGAAGC
<i>Caspase-3</i>	forward	GCGTAAGGAAAGGAGAGGTG
	reverse	ACAGACCAGTGCTCACAAGG
<i>Caspase-9</i>	forward	GGCCTTCACTTCCTCTCAAG
	reverse	GGACACAAGGATGTCACTGG
<i>Bcl-xl</i>	forward	ATGCAGGTATTGGTGAGTCG
	reverse	CCAAGGCTCTAGGTGGTCAT
<i>Bcl-2</i>	forward	TGCGACCTCTGTTGATTC
	reverse	GGTATGCACCCAGAGTGATG
<i>Bax</i>	forward	GATGGCAACTTCAACTGGG
	reverse	CCGAAGTAGGAGAGGAGGC
<i>AIF</i>	forward	TGCTTCAAGCAGAACTGG
	reverse	TCTAGAGAACACGCCATTG
<i>Fpn1</i>	forward	AATCGGTCTTGGTCCTTTG
	reverse	ATGCAGAACGGTCGAGAAGGT
<i>IL-10</i>	forward	GACGCTGTCATCGATTCTC
	reverse	TGGCCTTGAGACACCTTTG
<i>IL-6</i>	forward	AAGGACCAAGACCATCCAAC
	reverse	ACCACAGTAGGAATGTCCA
<i>IL-1β</i>	forward	GCATCCAGCTTCAAATCTCA
	reverse	ACGGGCAAGACATAGGTAGC
<i>Hmox1</i>	forward	ACCGCCTTCTGCTCAAC
	reverse	GAGGAGCGGTGTCTGGGAT
<i>Hsp70</i>	forward	CAAGAAGAACGGTCGTTGACA
	reverse	TTTCTCAGCCAGCGTGTAG
<i>Gapdh</i>	forward	GCACCGTCAAGGCTGAGAAC
	reverse	GTGGTGAAGACGCCAGTGGG

glutamyl transaminase (GGT), and alkaline phosphatase (ALP). The serum was examined at the First Affiliated Hospital of Nanchang University, China.

2.5 Histopathological examination

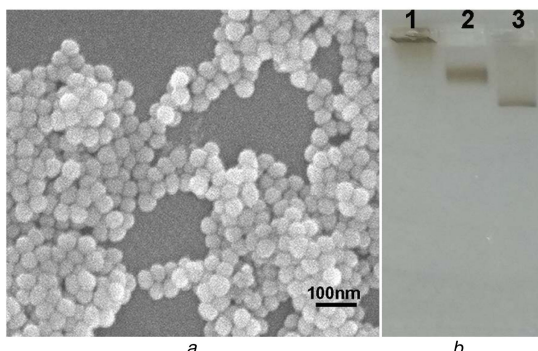
The liver was fixed in 10% neutral buffered formalin and was embedded in paraffin blocks (previously melted at 58°C). These were stored at 4°C before 4 µm sections were cut and stained with haematoxylin and eosin for histological examination. Each histology section were re-evaluated and semi-quantitatively scored by pathologist in Wuhan servicebio technology CO., LTD. The stained slices were observed by NIKON digital sight DS-F12.

2.6 RT-qPCR analysis

The liver plays an important role in metabolism, so the RNA from the liver collected from each group was extracted to elucidate whether there were corresponding gene expression changes from the various treatment groups. The total RNA was isolated using Takara MiniBEST Universal RNA extraction Kit (code no. 9767) according to the manufacturer's protocol. cDNA was synthesised using Takara PrimeScriptTM RT reagent kit (Cat#RR047A, Lot#AK2802) using 1 µg total RNA following the measured concentration of total RNA using a NanoDrop 1000 spectrophotometer (Thermo Scientific Inc.). RT-qPCR primers were synthesised by Invitrogen China (Shanghai, China) and Genscript China (Nanjing China), and are listed in Table 1. The gene encoding glyceraldehyde-3-phosphate dehydrogenase (Gapdh) was used as housekeeping gene. RT-qPCR was performed using SYBR[®] Premix Ex TaqTM II (TakaRa Code: DRR820A). Amplification was carried on a 7900HT Fast real-time System

Table 2 Particle characteristics of IOMNs

Particle type	Particle design	Hydrodynamic size, nm	Surface coating	Zeta potentials, mV
COOH-IOMNs	core/shell	51.2 ± 0.7	carboxylic acid	-36
PEG-IOMNs	core/shell	53.8 ± 0.51	PEG/carboxylic acid	+5.2
BSA-IOMNs	core/shell	62.4 ± 0.64	BSA/carboxylic acid	-31

**Fig. 1** Characterisation of the original particles (COOH-IOMNs)

(a) Image of SEM, (b) Migration in the 1% agarose gel, 1, PEG-IOMNs; 2, BSA-IOMNs; 3, COOH-IOMNs

(Applied Biosystems, Foster City, CA, USA) with the following two-step thermal cycling programme: 1 cycles at 95°C for 1 min, then 40 cycles of 95°C for 5 s, then 60°C for 1 min. Fold change of gene expression levels was determined using the critical threshold (C_t) number and calculated using the 2^{-ΔΔCt} method, with *Gapdh* as reference gene for all the test groups.

2.7 Statistical analysis

All the data were expressed as mean ± standard deviation and the comparison of results among the groups was carried out by one-way analysis of variance. Least significant difference test using SPSS v19.0 (SPSS, Inc., Chicago, IL, USA); **P* < 0.05 was considered statistically significant when compared with the control; ***P* < 0.01 was considered highly statistically significant when compared with the control.

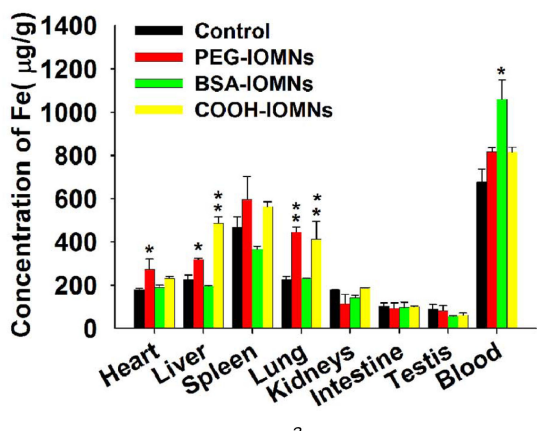
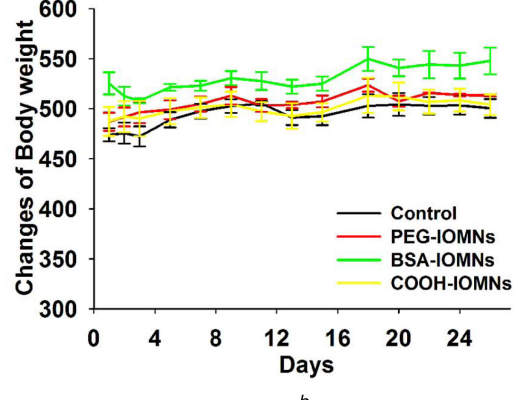
3 Results

3.1 Characterisation of IOMNs

As shown in Table 2, the hydrodynamic diameter of PEG-IOMNs, BSA-IOMNs, and COOH-IOMNs was 53.8 ± 0.51, 62.4 ± 0.64, and 51.2 ± 0.7 nm, respectively. Apart from the hydrodynamic sizes, the results indicated that PEG-IOMNs showed positive surface charge (+5.2), and BSA-IOMNs and COOH-IOMNs presented negative surface charge (-31 and -36, respectively). The morphology and size of COOH-IOMNs characterised by SEM (Fig. 1a) were consistent with previous results [6]. COOH-IOMNs showed fastest migration speed because of the more negative charge and lower molecular weight (Fig. 1b). The migration speed of PEG-IOMNs was slowest because of the positive charge.

3.2 Surface modification-dependent bio-distribution

The iron content in the kidneys, intestine, and testis did not show significant difference compared with the control group (Fig. 2a). PEG-IOMNs and COOH-IOMNs could be accumulated in the liver and lung. In addition, the iron contents in the spleen and blood were also elevated both in the PEG-IOMNs and COOH-IOMNs treatment group. The body weight of rats in different

*a**b***Fig. 2** Concentration of Fe in organs and body weight post-injection.

(a) Concentration of Fe (per gram of tissue) in various organs exposed to PEG-IOMNs, BSA-IOMNs, and COOH-IOMNs on day 24 post-injection
(b) Body weight following intravenous injection of various IOMNs, **P* < 0.05 versus the control group; ***P* < 0.01 versus the control group

treatment groups showed similar changes compared with the control group (Fig. 2b), and the rats administered with IOMNs showed no significance in the food intake and behaviour.

3.3 Biochemistry and histology results

On day 1 post-injection, the hepatic indicators (ALT, AST, TP, GLB, and A/G) values were significantly increased in both PEG-IOMNs (21.6, 125.9, 23.6, 24.8, and 69.5%, respectively) and COOH-IOMNs (62.2, 140.9, 34.8, 30.9, and 97.8%, respectively) groups (Fig. 3). In addition, COOH-IOMNs also increased the levels of other hepatic markers (ALB, 36.8%; ALP, 33.9%, and GGT, 50.0%) (Fig. 3). All the markers in the BSA-IOMNs treatment group were at the same level compared with the control group.

On day 9 or 16 post-injection, the hepatic indicators (ALT, AST, TP, ALB, GLB, GGT, DBIL, and TBIL) in BSA-IOMNs treatment group and the markers (ALT, AST, ALB, TP, GLB) in the COOH-IOMNs treatment group showed significant increase (Fig. 3). Nevertheless, only AST showed significant increase in the PEG-IOMNs treatment group on day 9 (33.2%) and day 16 (63.7%) post-injection (Fig. 3).

On day 24, all the markers in the COOH-IOMNs treatment group remained the same level as the control. However, PEG-IOMNs significantly increased hepatic indicators values (TP, 9.9%; GLB, 10.7%; ALT, 36.5%; AST, 32.9% and ALP, 119.7%) (Fig. 3). The indicators (ALT, 21.6%; AST, 47.4%; and ALP, 90.4%) in the BSA-IOMNs treatment group were also significantly increased (Fig. 3).

The hepatic lobule structure was clear in the four treatment groups, and cytoplasmic vacuolisation was observed in partial liver cells only in the PEG-IOMNs treatment groups. Furthermore, individual neutrophils in the local portal area were shown with

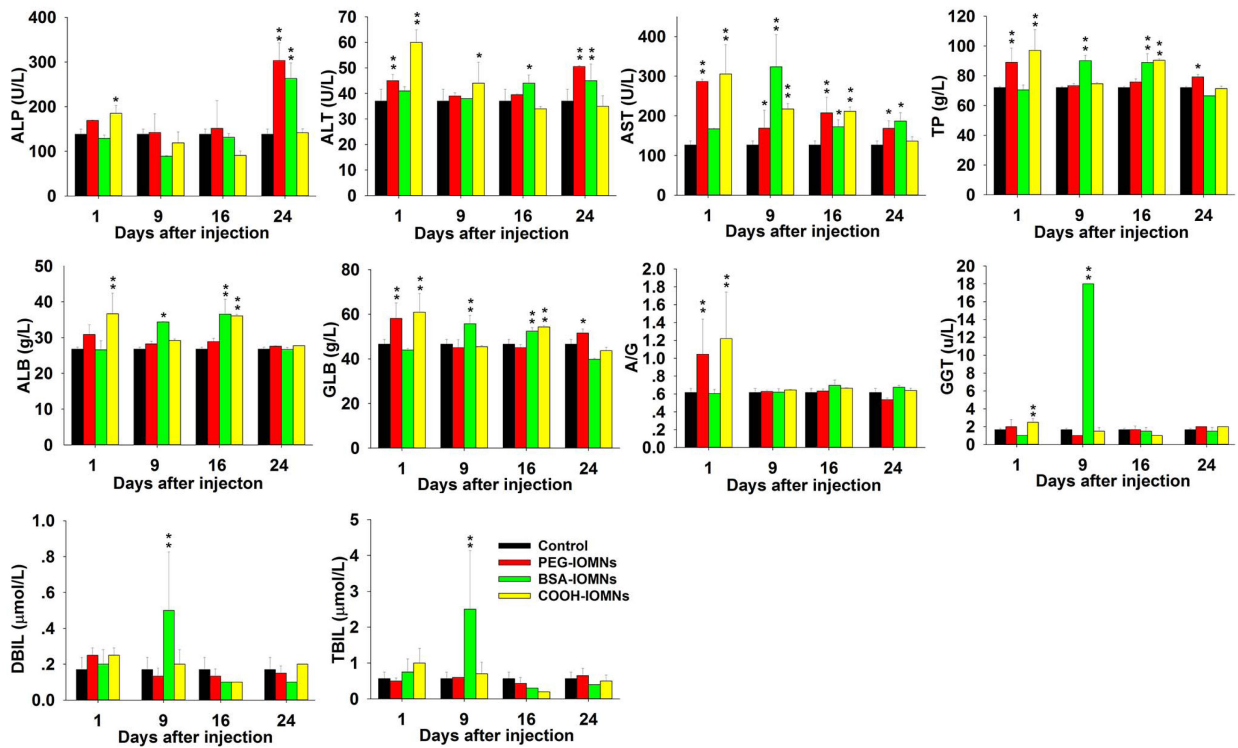


Fig. 3 Serum biochemical analysis of animals treated with various IOMNs at different time post-injection. * $P < 0.05$ versus the control group. ** $P < 0.01$ versus the control group

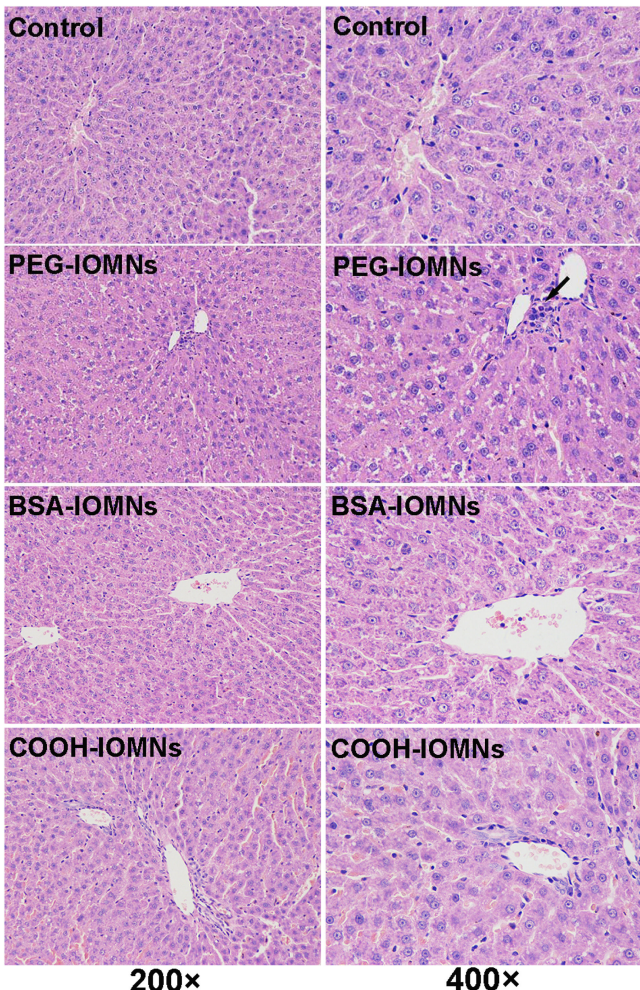


Fig. 4 Histological images (200 \times , 400 \times) of the liver collected from animals treated with various IOMNs and control on day 24 post-injection. The black arrow pointed the location of neutrophils in the local portal area

black arrowhead (Fig. 4). The semi-quantitative evaluation showed no obvious pathologic lesions (Table 3).

3.4 Gene expression evaluation

The cluster analysis of genic transcript level revealed similar transcription in the PEG-IOMNs and BSA-IOMNs treatment groups (Fig. 5a). The transcript level of genes related to apoptosis (Fig. 5b) including apoptosis-inducing factor (*AIF*), Cytochrome *c* (*Cytc*), apoptosis protease activating factor-1 (*Apaf-1*), *Caspase-8*, *Caspase-9*, and *Bcl2*-associated *X* protein (*Bax*) were up-regulated, while the *Bcl2*-like 1 isoform 1 (*Bcl-xL*) were down-regulated in all the treatment groups. *Caspase-3* and *Bcl-2* showed up-regulation in COOH-IOMNs. The up-regulation of *Ferroportin1* (*Fpn1*) related to iron homeostasis, anti-inflammatory factor [*Interleukin-10* (*IL-10*)], and *heat shock protein 70* (*Hsp70*) were observed in the three treatment groups, while pro-inflammatory factor including *interleukin-6* (*IL-6*) and *interleukin-1 β* (*IL-1 β*) were down-regulated in the three treatment groups (Fig. 5c). *Heme oxygenase 1* (*Hmox1*) related to antioxidant showed up-regulation in the COOH-IOMNs group. However, the expression changes are below a 2-fold change in comparison to control in most of the cases.

4 Discussion

NPs can be identified by innate immune system after intravenous injection, affecting the distribution and drug targeting transport [7, 8]. With the help of surface modification, IOMNs were not efficiently taken up by macrophages, prolonging the circulation time of IOMNs *in vivo* [1, 25, 26]. However, IOMNs coated with functional materials can still induce side effects. To evaluate and compare the possible side effects of IOMNs with different surface modification, we evaluated the toxicity of three types of IOMNs in this work.

After 24 day recovery, IOMNs were still found in different organs, and showed different patterns of IOMNs accumulation in the heart, liver, spleen, lung, and blood (Fig. 2), which suggested that surface modification can affect the distribution of IOMNs and was helpful for targeting distribution of IOMNs. Muthiah *et al.* [27] demonstrated that SPIONs with functionalised surface can accumulate more efficiently in the tumour or specific region in the literature review. Xu *et al.* [28] also revealed that high PEG surface

density may be effective for drug delivery. In addition, BSA-coated IOMNs showed fewer accumulation *in vivo*, and more accumulation in blood than PEG-IOMNs and COOH-IOMNs, which indicated that naturally occurring compound, such as BSA, were more suitable for surface modification. Meanwhile, another naturally occurring compound, adenosine triphosphate (ATP), also prolonged the circulation of SPIONs in the blood, and showed fewer uptake by the liver [9].

The liver was important for metabolism and was the main organ where IOMNs accumulated [6, 17]. Within the first day, representative serum biomarkers were enhanced in the PEG-IOMNs and COOH-IOMNs treatment groups, except BSA-IOMNs treatment group (Fig. 3). This result indicated that the BSA-IOMNs may have less acute toxicity on liver compared with PEG-IOMNs and COOH-IOMNs. Based on the change of hepatic serum biochemical markers on days 9, 16, and 24, PEG-IOMNs, BSA-IOMNs, and COOH-IOMNs seemed to have side effect on hepatic function. Furthermore, individual neutrophils and cytoplasmic vacuolisation was observed in partial liver cells of the PEG-IOMNs treatment group (Fig. 4) indicated that IOMNs with surface coating might induce toxicity on the liver with the longer existence of IOMNs *in vivo*. Also, the histology results were consistent with the result that PEG-IOMNs might have higher acute toxicity than BSA-IOMNs. Interestingly, vascular congestion, necrosis, and inflammatory infiltrate in the liver and kidney were also found on the 14th day after intravenous administration in previous study [13]. The results in this work were consistent with the conclusion that IOMNs coated with function materials can still induce side effects [11–14].

In addition, the difference of iron content in the PEG-IOMNs and BSA-IOMNs treatment groups did not lead to the different genic transcript levels (Figs. 2a and 5a). To further investigate the transcript levels in different groups, fold change of transcript levels in comparison to control were analysed (Figs. 5b and c).

As iron content in the PEG-IOMNs and COOH-IOMNs treatment groups showed 42.5 and 116.7% increase compared with the control. IOMNs may release iron ions and affect the iron balance. *Fpn1* acted as an exporter that recycled iron from senescent red blood cells and exported iron out of the cell, maintaining the iron homeostasis [29, 30]. The up-regulation of *Fpn1* in three treatment groups indicated that IOMNs may induce iron homeostasis of the liver. In addition, the up-regulation of *Hsp70* indicated that defensive function in response to IOMNs was activated in the liver [31], which can also be confirmed by the transcript levels of pro-inflammatory factor (*IL-6*, *IL-1 β*) and anti-inflammatory factor (*IL-10*) [32]. Though *Hsp70* showed lower transcript levels in the COOH-IOMNs groups than that in the PEG-IOMNs and BSA-IOMNs groups, COOH-IOMNs induced higher anti-inflammatory and antioxidant activity than PEG-IOMNs and BSA-IOMNs.

Owing to the great application prospect in biomedicine, whether IOMNs can induce normal cell apoptosis or not is necessary to investigate. Apoptotic pathways consisted of extrinsic receptor-mediated pathway and intrinsic pathway. Mitochondria played a major role in the intrinsic apoptotic pathway [33]. Moreover, mitochondrial apoptosis was a pathway to kill cancer cell [34]. Caspase protease activity was essential for apoptosis, and caspase activity can be initiated through the mitochondria-mediated pathway. Cyt c could be released into the cytosol following the mitochondrial outer membrane permeabilisation. Cyt c in the cytosol binded the adaptor molecule Apaf-1 activating caspase-9, and then activated the executioner caspases-3. Cells were killed by

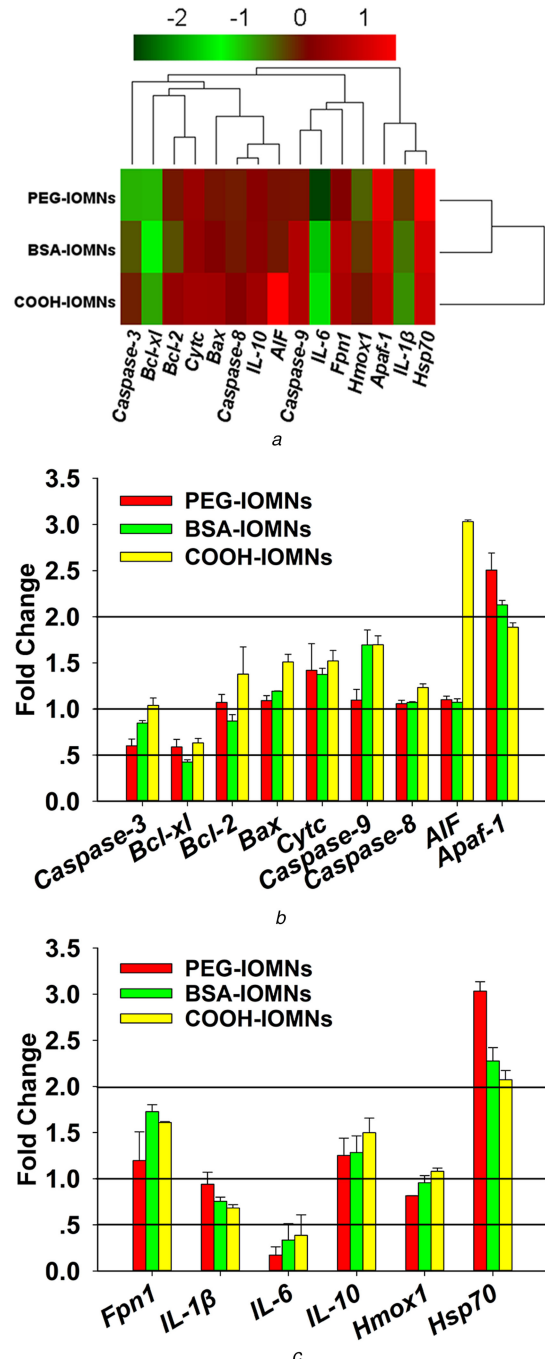


Fig. 5 The genic transcript level in PEG-IOMNs, BSA-IOMNs, and COOH-IOMNs treatment groups.

(a) Initial screening of gene relative expression of animals treated with PEG-IOMNs, BSA-IOMNs, and COOH-IOMNs in the liver. Quantitative real-time PCR was used to analyse the transcriptional response. Red samples represent up-regulated mRNAs, whereas green samples represent down-regulated mRNAs. Data are presented as log₂-transformed fold change (fold change = $2^{-\Delta\Delta Ct}$ value), (b, c) Change in gene expression in the liver on day 24 post-injection. The changed value was presented as a $2^{-\Delta\Delta Ct}$ value in the histogram. The ratio which was greater than zero indicates up-regulation of gene expression, whereas the ratio below zero indicates down-regulation

Table 3 Semi-quantitative score of histology evaluation in rats liver tissues

Groups	necrosis	inflammation	haemorrhage	degeneration	fibrosis
control	0	0	0	0	0
PEG-IOMNs	0	0	0	0	0
BSA-IOMNs	0	0	0	0	0
COOH-IOMNs	0	0	0	0	0

According to the degree of pathological changes from mild to severe degree, 1, mild or very little ‘±’; 2, mild or small ‘+’; 3, moderate or moderate amount of ‘++’; 4, severe or large amount of ‘+++’; 5, large number or extremely severe ‘++++’; 0, no lesions.

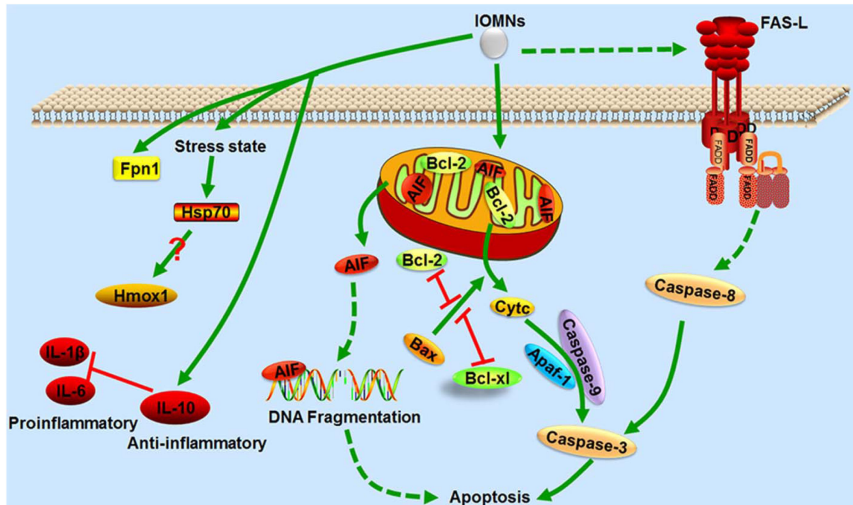


Fig. 6 Schematic representation of the proposed mechanism for COOH-IOMNs treatment activates the mitochondria apoptosis and induces stress response

executioner caspase-3 within minutes. In this process, Bcl-2 protein family including pro-apoptotic effector proteins (Bax) and anti-apoptotic Bcl-2 proteins (Bcl-2, Bcl-xL) were related to the release of Cytc [34, 35]. Bax can promote apoptosis by inducing the release of Cytc, whereas Bcl-xL and Bcl-2 can inhibit apoptosis by counteracting the effects of Bax and acting downstream of Cytc in the cell death pathway [36]. Owing to the up-regulation of pro-apoptotic Bcl-2 family gene (*Bax*) and the inhibition effect of Bax, only one anti-apoptotic Bcl-2 family gene (*Bcl-xL*) showed up-regulation in the PEG-IOMNs and COOH-IOMNs groups. This result was beneficial to the release of Cytc. Furthermore, the up-regulation of marker genes (*Cytc*, *Caspase-9*, *Apaf-1*) indicated that the mitochondrial apoptotic pathway may be activated. However, *Caspase-3* was up-regulated only in the CCOH-IOMNs treatment group, and the up-regulation was not significant. We suggested that though the *Bax*, *Cytc*, and *Caspase-9* were up-regulated, their transcript levels and expression were still low (<2-fold alteration), which cannot activate Caspase-3 effectively. Analogously, Caspase-8 which can also activate Caspase-3 through the adaptor protein Fas-associated death domain pathway [37] was also up-regulated <2-fold alteration. Through these two pathways, only COOH-IOMNs induced the up-regulation of *Caspase-3*. Furthermore, AIF can also be released from the mitochondria and subsequently localised to the nucleus, which can induce apoptosis by breaking double-stranded DNA and condensing large-scale DNA in the absence of caspase activity [38]. This result showed that only COOH-IOMNs induced >2-fold increase in transcript levels of *AIF*. In most of the cases, the expression changes were below a 2-fold change in comparison to control. IOMNs coated with BSA and PEG may not promote normal cell apoptosis. Schematic representation of the proposed mechanism for COOH-IOMNs treatment activates the mitochondria apoptosis and induces stress response (Fig. 6).

5 Conclusion

Our study demonstrated that surface modifications played an important role in the bio-distribution of IOMNs. After 24 day recovery, BSA-IOMNs had longer-term retention time in blood, and PEG-IOMNs seemed to have more accumulation in various organs than BSA-IOMNs. PEG-IOMNs, BSA-IOMNs, and COOH-IOMNs can still have side effects on liver function. Compared with PEG-IOMNs and COOH-IOMNs, PEG-IOMNs also induced individual neutrophils and cytoplasmic vacuolization in partial liver cells. Though most genes related to mitochondrial apoptosis were up-regulated, the alteration were <2-fold. In addition, COOH-IOMNs can induce normal cell apoptosis more easily than PEG-IOMNs and BSA-IOMNs through the mitochondria-mediated pathway.

6 Acknowledgments

This work was supported by Natural Science Foundation of China (81560537), Training Plan for the Young Scientist (Jinggang Star) of Jiangxi Province (20142BCB23004), and Major Program of Natural Science Foundation of Jiangxi Province (20143ACB21003). The authors would like to thank Dr Andrew Wang and Dr Hong Xu for providing valuable information and the materials of the IOMNs.

7 References

- [1] Liu, G., Gao, J., Ai, H., et al.: 'Applications and potential toxicity of magnetic iron oxide nanoparticles', *Small*, 2013, **9**, (9–10), pp. 1533–1545
- [2] Xu, H., Aguilar, Z.P., Yang, L., et al.: 'Antibody conjugated magnetic iron oxide nanoparticles for cancer cell separation in fresh whole blood', *Biomaterials*, 2011, **32**, (36), pp. 9758–9765
- [3] Valdiglesias, V., Kilic, G., Costa, C., et al.: 'Effects of iron oxide nanoparticles: cytotoxicity, genotoxicity, developmental toxicity, and neurotoxicity', *Environ. Mol. Mutagen.*, 2015, **56**, (2), pp. 125–148
- [4] Sarkar, A., Sil, P.C.: 'Iron oxide nanoparticles mediated cytotoxicity via PI3k/Akt pathway: Role of quercetin', *Food chem. Toxicol.*, 2014, **71**, pp. 106–115
- [5] Hanini, A., Schmitt, A., Kacem, K., et al.: 'Evaluation of iron oxide nanoparticle biocompatibility', *Int. J. Nanomedicine*, 2011, **6**, pp. 787–794
- [6] Yang, L., Kuang, H., Zhang, W., et al.: 'Size dependent biodistribution and toxicokinetics of iron oxide magnetic nanoparticles in mice', *Nanoscale*, 2015, **7**, (2), pp. 625–636
- [7] Asadi, H., Khoee, S., Deckers, R.: 'Polymer-grafted superparamagnetic iron oxide nanoparticles as a potential stable system for magnetic resonance imaging and doxorubicin delivery', *RSC Adv.*, 2016, **6**, (87), pp. 83963–83972
- [8] Inturi, S., Wang, G., Chen, F., et al.: 'Modulatory role of surface coating of superparamagnetic iron oxide nanoworms in complement opsonization and leukocyte uptake', *ACS Nano*, 2015, **9**, (11), pp. 10758–10768
- [9] Lee, C.-M., Cheong, S.-J., Kim, E.-M., et al.: 'Nonpolymeric surface-coated iron oxide nanoparticles for in vivo molecular imaging: biodegradation, biocompatibility, and multiplatform', *J. Nucl. Med.*, 2013, **54**, (11), pp. 1974–1980
- [10] Dolci, S., Domenici, V., Vidili, G., et al.: 'Immune compatible cysteine-functionalized superparamagnetic iron oxide nanoparticles as vascular contrast agents in ultrasonography', *RSC Adv.*, 2016, **6**, (4), pp. 2712–2723
- [11] Xu, Y., Sherwood, J.A., Lackey, K.H., et al.: 'The responses of immune cells to iron oxide nanoparticles', *J. Appl. Toxicol.*, 2016, **36**, (4), pp. 543–553
- [12] Nora, N.A.M., Ridwana, R., Che, N.: 'In vivo assessment on acute toxicity of iron oxide nanoparticles with different coatings', *Apoptosis*, 2016, **11**, p. 13
- [13] Silva, A.H., Lima, E., Mansilla, M.V., et al.: 'Superparamagnetic iron-oxide nanoparticles mpeg350- and mpeg2000-coated: cell uptake and biocompatibility evaluation', *Nanomedicine*, 2016, **12**, (4), pp. 909–919
- [14] Easo, S.L., Mohanan, P.: 'Hepatotoxicity evaluation of dextran stabilized iron oxide nanoparticles in wistar rats', *Int. J. Pharm.*, 2016, **509**, (1), pp. 28–34
- [15] Mohanty, A.K., Dilnawaz, F., Mohanta, G.P.: 'Polymer-drug conjugates for targeted drug delivery', in Devarajan, P., Jain, S. (Eds.): 'Targeted drug delivery: concepts and design' Advances in Delivery Science and Technology. (Springer, Cham, 2015), pp. 389–407
- [16] Yu, C., Al-Saadi, A., Shih, S.J., et al.: 'Immobilization of BSA on silica-coated magnetic iron oxide nanoparticle', *J. Phys. Chem. C*, 2008, **113**, (2), pp. 537–543
- [17] Cole, A.J., David, A.E., Wang, J., et al.: 'Magnetic brain tumor targeting and biodistribution of long-circulating peg-modified, cross-linked starch-coated iron oxide nanoparticles', *Biomaterials*, 2011, **32**, (26), pp. 6291–6301
- [18] Ruiz, A., Hernandez, Y., Cabal, C., et al.: 'Biodistribution and pharmacokinetics of uniform magnetite nanoparticles chemically modified with polyethylene glycol', *Nanoscale*, 2013, **5**, (23), pp. 11400–11408

- [19] Mahmoudi, M., Sant, S., Wang, B., *et al.*: 'Superparamagnetic iron oxide nanoparticles (SPIONs): development, surface modification and applications in chemotherapy', *Adv. Drug. Deliv. Rev.*, 2011, **63**, (1-2), pp. 24–46
- [20] Mikhaylova, M., Kim, D.K., Berry, C.C., *et al.*: 'BSA immobilization on amine-functionalized superparamagnetic iron oxide nanoparticles', *Chem. Mater.*, 2004, **16**, (12), pp. 2344–2354
- [21] Tran, T.T.-D., Van Vo, T., Tran, P.H.-L.: 'Design of iron oxide nanoparticles decorated oleic acid and bovine serum albumin for drug delivery', *Chem. Eng. Res. Des.*, 2015, **94**, pp. 112–118
- [22] Elzoghby, A.O., Samy, W.M., Elgindy, N.A.: 'Albumin-based nanoparticles as potential controlled release drug delivery systems', *J. Control. Release*, 2012, **157**, (2), pp. 168–182
- [23] Aires, A., Ocampo, S.M., Cabrera, D.: 'BSA-coated magnetic nanoparticles for improved therapeutic properties', *J. Mater. Chem. B*, 2015, **3**, (30), pp. 6239–6247
- [24] Prabhu, S., Matalik, S., Rai, S.: '
- [25] Amstad, E., Textor, M., Reimhult, E.: 'Stabilization and functionalization of iron oxide nanoparticles for biomedical applications', *Nanoscale*, 2011, **3**, (7), pp. 2819–2843
- [26] Ling, D., Lee, N., Hyeon, T.: 'Chemical synthesis and assembly of uniformly sized iron oxide nanoparticles for medical applications', *Acc. Chem. Res.*, 2015, **48**, (5), pp. 1276–1285
- [27] Muthiah, M., Park, I.K., Cho, C.S.: 'Surface modification of iron oxide nanoparticles by biocompatible polymers for tissue imaging and targeting', *Biotechnol. Adv.*, 2013, **31**, (8), pp. 1224–1236
- [28] Xu, Q., Ensign, L.M., Boylan, N.J.: 'Impact of surface polyethylene glycol (PEG) density on biodegradable nanoparticle transport in mucus ex vivo and distribution in vivo', *ACS Nano*, 2015, **9**, (9), pp. 9217–9227
- [29] Zhang, Z., Zhang, F., Guo, X.: 'Ferroportin1 in hepatocytes and macrophages is required for the efficient mobilization of body iron stores in mice', *Hepatology*, 2012, **56**, (3), pp. 961–971
- [30] Drakesmith, H., Nemeth, E., Ganz, T.: 'Ironing out ferroportin', *Cell Metab.*, 2015, **22**, (5), pp. 777–787
- [31] Liu, D., Ma, L., Liu, L.: 'Polydopamine-encapsulated Fe₃O₄ with an adsorbed Hsp70 inhibitor for improved photothermal inactivation of bacteria', *ACS Appl. Mater. Inter.*, 2016, **8**, (37), pp. 24455–24462
- [32] Flemming, A.: 'Autoimmunity: nanoparticles engineered for antigen-specific immunotherapy', *Nat. Rev. Immunol.*, 2016, **16**, (4), pp. 204–205
- [33] Patwardhan, G.A., Beverly, L.J., Siskind, L.J.: 'Sphingolipids and mitochondrial apoptosis', *J. Bioenerg. Biomembr.*, 2016, **48**, (2), pp. 153–168
- [34] Lopez, J., Tait, S.: 'Mitochondrial apoptosis: killing cancer using the enemy within', *Brit. J. Cancer*, 2015, **112**, (6), pp. 957–962
- [35] Renault, T.T., Dejean, L.M., Manon, S.: 'A brewing understanding of the regulation of bax function by Bcl-XL and Bcl-2', *Mech. Ageing Dev.*, 2017, **161**, pp. 201–210
- [36] Siddiqui, W.A., Ahad, A., Ahsan, H.: 'The mystery of Bcl2 family: Bcl-2 proteins and apoptosis: an update', *Arch. Toxicol.*, 2015, **89**, (3), pp. 289–317
- [37] Creagh, E.M.: 'Caspase crosstalk: integration of apoptotic and innate immune signalling pathways', *Trends. Immunol.*, 2014, **35**, (12), pp. 631–640
- [38] Milasta, S., Dillon, C.P., Sturm, O.E.: 'Apoptosis-inducing-factor-dependent mitochondrial function is required for T cell but not B cell function', *Immunity*, 2016, **44**, (1), pp. 88–102